



TITLE:

# On the Multiple Structure in the K X-ray Absorption Spectra of the Metallic Elements Cr, Mn, Fe, Co, Ni and Cu

AUTHOR(S):

Sawada, Masao

---

CITATION:

Sawada, Masao. On the Multiple Structure in the K X-ray Absorption Spectra of the Metallic Elements Cr, Mn, Fe, Co, Ni and Cu. *Memoirs of the College of Science, Kyoto Imperial University. Series A* 1931, 14(5): 229-250

ISSUE DATE:

1931-09-30

URL:

<http://hdl.handle.net/2433/256973>

RIGHT:

# On the Multiple Structure in the $K$ X-ray Absorption Spectra of the Metallic Elements Cr, Mn, Fe, Co, Ni and Cu

By

Masao Sawada

(Received August 7, 1931)

---

## Abstract

An extended multiple structure of the  $K$  X-ray absorption spectra of the metallic elements Cr, Mn, Co, Fe, Ni and Cu has been photographed.

Some of them extend over an energy range of more than 400 volts.

Throughout the work, the absorbing media were pure metallic elements.

They were prepared by the method of electrodeposition and in the case of manganese the evaporation method was chosen, with a specially designed apparatus.

For copper, in addition to the plates taken with an extra metallic screen, a single-crystal of copper served as the analyser and also as the absorber.

The spectrograms and the microphotometer curves of them are shown.

Several views to account for the origin of the extended multiple structure have been proposed by investigators, but here two hypotheses were taken into consideration and compared with the experimental data.

The first hypothesis considered was that of multiple electron transitions due to the absorption of a quantum of X-rays.

The second was that of the ejection of a  $K$ -electron from the multiply ionized atom in various shells.

In accordance with the first hypothesis, the energy level diagram for multiple X-ray ionization was constructed on the assumption that the  $\{jj\}$  coupling of electrons holds. The intersections of the curves of multiple ionization of different degree are interesting compared with the experimental curves. Of course some discrepancies between the calculated and observed value may be expected owing to the change in electron coupling from  $\{jj\}$  to  $\{LS\}$ . This point is discussed, use being made of the recently published results of S. Goudsmit.

In accordance with the second hypothesis, some calculations were made by extending Wentzel's work. The experimental fact that the slow change of the value of  $\frac{\nu}{K}$  with the atomic number of the corresponding lines of similar intensity and structure are favourable to this view. But there remains a theoretical question of the new quantum mechanics as to which of the processes suggested by the two hypotheses most frequently occurs.

As a whole, the most probable explanation seems to be that two such phenomena occur in the process of absorption of X-rays.

### Introduction

DURING the last few years a very complicated, "fine structure" or "multiple structure" of the short wave-length side of the edge of the X-ray absorption spectra has been investigated.

In an investigation of the absorption spectra of calcium, using a crystal containing the element both as a diffracting crystal and as an absorbing medium, Lindsay and Van Dyke<sup>1</sup> obtained four secondary edges.

But the explanation of this was not satisfactory. In the case of elements of low atomic number, the valency of the element affects the position of the absorption edge, and we have no sure knowledge of the terms of lower levels. In consideration of this, I chose a copper single-crystal<sup>2</sup> as an analyser and an absorber, and obtained as many as five secondary edges, as shown in Fig. 2 (A) (Plate), and put forward the explanation<sup>3</sup> that these were the absorption edges corresponding to the simultaneous removal of the *K* and *M* electrons of copper. At about the same time, Nuttal<sup>4</sup> got similar results for potassium and chlorine in chemical compounds.

Later, many researches were made in the same direction.

For example;

Lindsay and Voorhees<sup>5</sup> (Iron: metallic element, and many of its chemical compounds)

Meyer<sup>6</sup> (Bromine: Bromate)

Coster<sup>7</sup> (Copper: metallic element)

Lindh<sup>8</sup> (Copper and nickel: metallic element)

Recently B. Kievit, and G. A. Lindsay<sup>9</sup> obtained many secondary edges for the metallic elements Zn, Cu, Ni, Fe, Co, Cr, and Ca and also for Mn-alloy. And on the basis of multiple ionization the probable transitions of the electrons have been determined to account for them.

1. G. A. Lindsay and G. Van Dyke, *Phys. Rev.* **27**, 508 (1926)

2. This sample was kindly prepared in the laboratory of Prof. Yoshida by Mr. S. Takeyama.

3. M. Sawada, in a paper read at the meeting of our seminary.

4. J. M. Nuttal, *Phys. Rev.* **31**, 742 (1928)

5. G. A. Lindsay and H. R. Voorhees, *Phil. Mag.* **6**, 910 (1928)

6. H. T. Meyer, *Wiss. Veröff. a. d. Siemens-Konzern VII* **2**, 101 (1929)

7. D. Coster, *Nature* **124**, 652 (1929)

8. A. E. Lindh, *Zeits. für Physik*, **63**, 106 (1930)

9. B. Kievit and G. A. Lindsay, *Phys. Rev.* **36**, 648 (1931)

I have studied the same range of elements and their compounds since 1928, and the part of my investigation dealing with the metallic elements from Cu (29) to Cr (24) inclusive will be here described.

## Part I. Experimental

### (I) The X-ray Apparatus

For obtaining spectrograms of the absorption edges, a Seemann's "edge" vacuum spectrograph was used. The X-ray tube attached to it was a modified large electron tube of Siegbahn type, constructed in this laboratory. A calcite crystal served as a reflector and was continuously rotated through an angle of about  $2.5^\circ$  around the wavelength in question. The current through the tube was about 20 milliamperes, the time of exposure<sup>1</sup> varying from 50 to 100 hours. The voltage applied to the tube was supplied by a large induction coil and was regulated so as to prevent the excitation of second-order emission lines in the region under investigation.

The X-ray tube was evacuated by a Gaede three-stage steel pump, preceded by an oil pump. A thin aluminium foil covered the window of the tube, and separated it from the vacuum spectrograph, which was evacuated by the oil pump alone.

### (II) The Preparation of the Absorbing Screens

The problem of obtaining absorbing screens of suitable thickness (thinner than 0.01 m.m.) for the best photographic impression of the multiple structure of the absorption limit is experimentally a difficult matter.

In the investigation here reported they were prepared by the method of electrodeposition or evaporation.

1. NICKEL. The solution of electrolyte which was used had the following composition: nickel sulphate 125 gms., ammonium chloride 17 gms., boric acid 15 gms., and water 1000 c.c. This was used at a temperature of about  $23^\circ\text{C}$ , with a current density of 0.7 amps. per  $\text{dm}^2$ . A thin copper plate was immersed in the  $\text{K}_2\text{Cr}_2\text{O}_7$  solution, then within quite a short time an imperceptible film of oxide was formed, and this plate was then coated with nickel. Stripping was most likely to occur, and it occurred very markedly.

---

1. Only 20 hours in the case of copper single-crystal.

2. COBALT. To a solution of sulphate of cobalt (cryst.) containing 25 gms. of the salt per 50 gms. of water, 0.85 gm. sodium chloride and 2.25 gms. boric acid were added and dissolved. A current density of 1.1 amps. per  $\text{dm}^2$  and a temperature ranging from  $20^\circ$  to  $25^\circ\text{C}$  was used. The deposit from this solution on a chromium plated copper electrode was very bright, and of a brilliant white colour.

The deposited cobalt film could be stripped from the electrode by heating it gently.

3. IRON. The electrolyte was composed of 600 gms. ferrous chloride and 670 gms. calcium chloride per liter of water. A temperature of about  $100^\circ\text{C}$  and a current density of 10 amps. per  $\text{dm}^2$  was used.

The anode was of platinum. Iron was deposited on zinc plate and after slightly heating it could be peeled off, yielding smooth, dense films that could be handled without danger of breaking.

4. CHROMIUM. In this case the electrolyte was a solution composed of 200 gms. chromic acid per liter of water used at room temperature with a current density of 50 amps. per  $\text{dm}^2$ . The method of deposition on copper followed by removal of the copper by dissolving it in dilute nitric acid was only partly successful, the thin film of chromium being broken by the weight of the residual copper itself, on account of the irregular etching of the copper by the acid. The next method tried was one in which a very thin sheet of copper was thinly chromium plated and after rinsing in water, this was again dipped into the copper plating vat, and received over it a thin coating of copper. This was followed by slight annealing and then the copper was dissolved in dilute nitric acid. Finally a very good brilliant chromium screen was obtained.

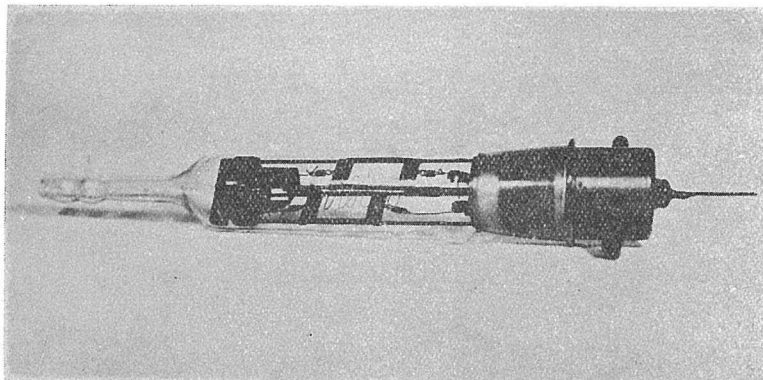
5. MANGANESE. The production of uniform manganese screens of the required thickness was difficult. Many attempts were made; (1) by cathodic sputtering, (2) by electrodeposition on Wood's alloy, and so on. Finally the evaporation method was chosen as the best one.

The essential feature of the evaporation method of obtaining a film is the moving of two aluminium foils back and forth one above and the other below an electrically heated filament of the metal under investigation. The particles of metal given off by the hot filament adhere to the foil, giving uniform film. The details of the evaporation apparatus are shown in Fig. 1.

Two sets of two steel rails are fitted into a brass disc and a water-cooled conical brass ground joint. Two brass frames, which can hold an aluminium foil, constitute the carriage. Through the centre

Fig. 1

The evaporation apparatus.



of the conical ground joint, a steel wire protrudes and serves as an electrode and also a holder of a tungsten filament, upon which manganese was coated by electrodeposition<sup>1</sup>.

The electromagnet turns around the glass tube. The small piece of iron turns with the magnet. By means of a small capstan, the carriage is drawn along the rails. Thus the carriage moves back and forth along the rails.

The tube was connected to a Gaede three-stage steel pump, with an oil pump as fore-pump. The minimum distance of the wire from the aluminium foil was less than the mean free path of the gas molecules.

Evaporated manganese was found to be very bright and uniform in thickness. This served as an absorber and as a window for the X-ray tube.

### (III) Measurements

In measuring the absorption edge of the spectrogram by the comparator the cross hair of a microscope of low magnifying power was brought up to the points where the blackening begins to increase and also to disappear. This was very difficult, and especially for the faint and diffuse edge comparatively large errors might be introduced.

The width of the slit was 0.025 m.m. and no correction due to it was made. The computation of the wave-length of edges or lines was as follows :

---

1. Handb. d. exp. Phys. Bd. 1, 463 (1926)

Let  $a$  be the separation between two reference lines  $\lambda_1$ , and  $\lambda_2$ , and  $\Delta\alpha$  that between the required wave-length  $\lambda$  and  $\lambda_2$ ; and let the glancing angle of wave-lengths  $\lambda_1, \lambda_2, \lambda$  be  $\theta_1, \theta_2, \theta$  respectively; then, we have

$$\tan \theta = \tan \theta_2 - \frac{\Delta\alpha}{a} (\tan \theta_2 - \tan \theta_1).$$

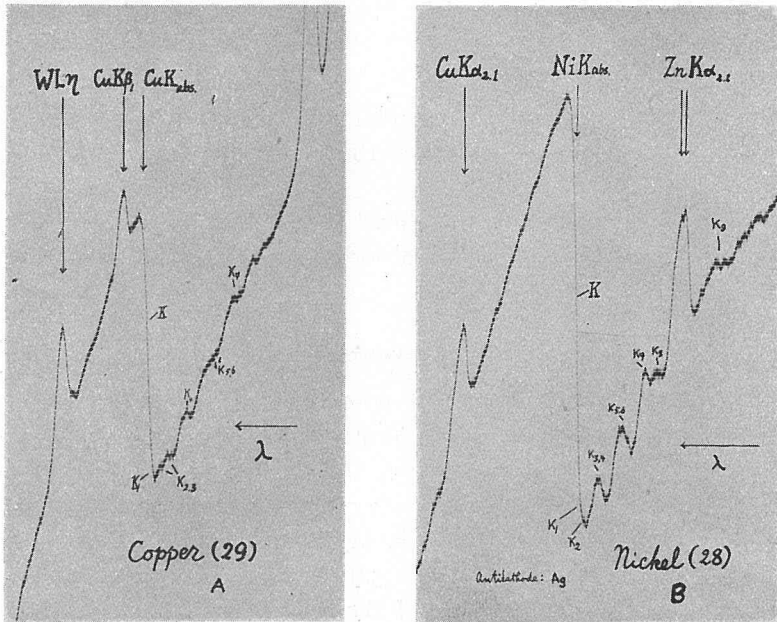
The evaluation of wave-lengths is accomplished by means of Bragg's formula. But in using the preceding formula the reflecting crystal and the X-ray plate must be perpendicular to each other.

#### (IV) The Microphotometric Records

The curves shown in Figs. 3 (A)-(K) are microphotographs taken with a Moll-microphotometer<sup>1</sup>. They served as the check for the wave-length determination and also for showing general views of the spectrogram. Figs. 3. (C), (E), (G) and (K) were taken with a somewhat narrow slit than the others.

Fig. 3 (A)-(B)

Microphotometric records of the multiple structure in the K absorption spectra.



1. The author wishes to express his thanks to Mr. E. Kasai for his kind help in preparing the curves.

Fig. 3 (C)—(E)

Microphotometric records of the multiple structure in the K absorption spectra.

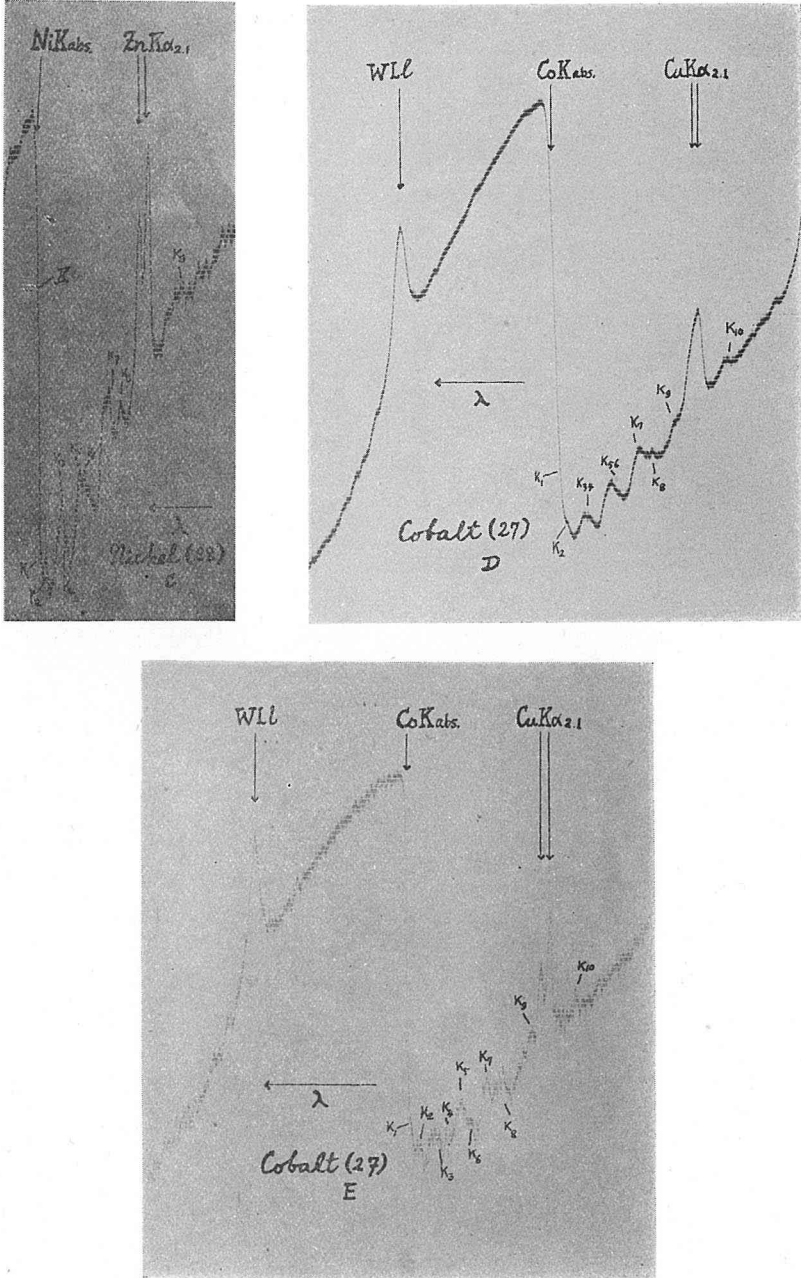




Fig. 3 (F)–(H)

Microphotometric records of the multiple structure in the K absorption spectra.

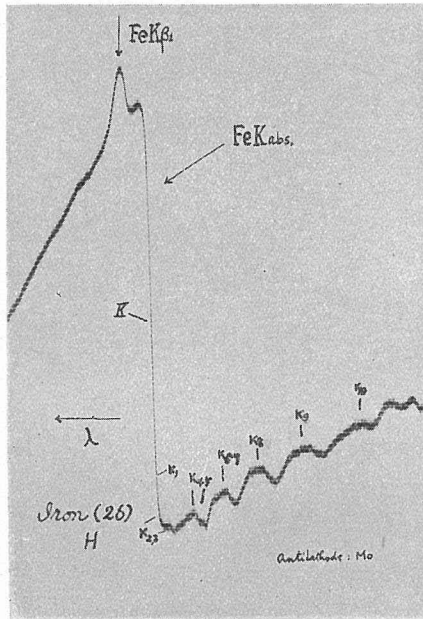
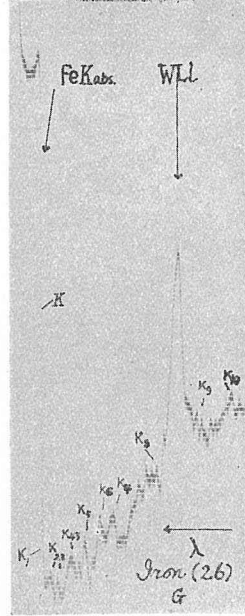
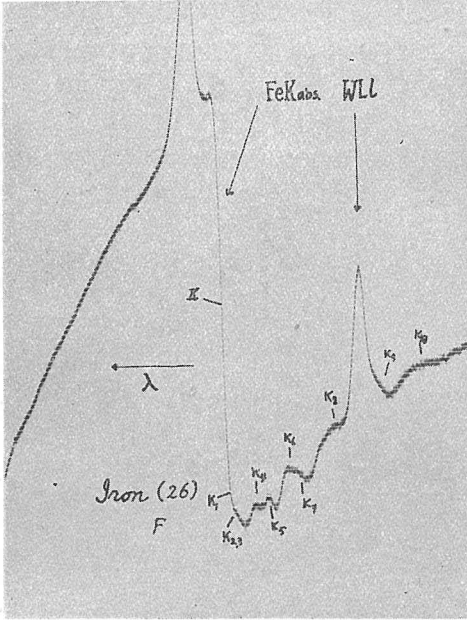
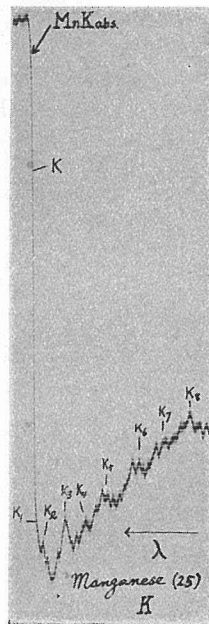
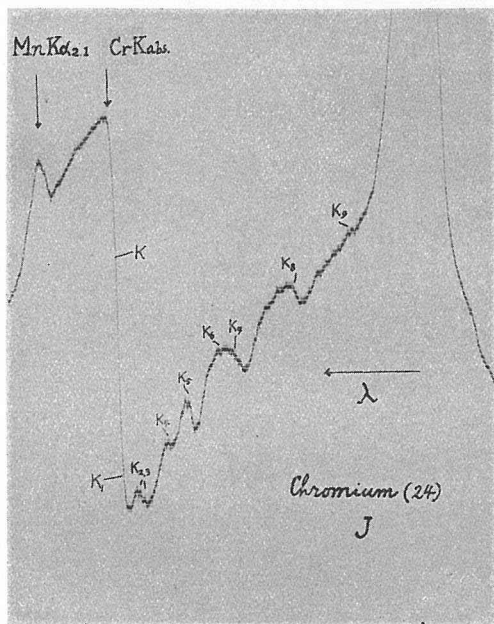
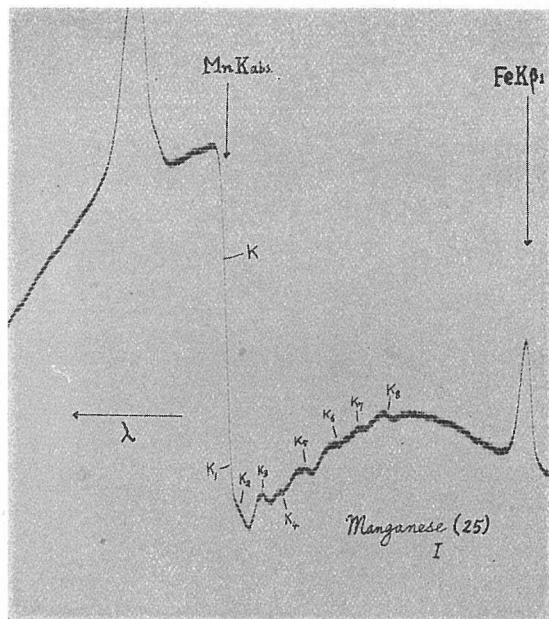


Fig. 3 (I)–(K)

Microphotometric records of the multiple structure in the K absorption spectra.



## (V) The Spectrograms

Reproduction of the spectrograms are given in Fig. 2 (Plate).

The materials of the anticathode and the cathode and the wave-lengths of the reference lines are given in Table I.

Table I

Spectro-gram	Element	Anticathode	Cathode	Reference Lines
Fig. 2 (B)	Cu (29)	Tungsten	Tungsten	WZ $\eta$ $\lambda=1418.10$ , WZ $\beta$ , $\lambda=1279.17$
" (C)	Ni (28)	Silver	An oxide-coated platinum filament	CuK $\alpha_2$ , $\lambda=1541.16$ , ZnK $\alpha$ , $\lambda=1432.06$
" (D)	Co (27)	Tungsten	Tungsten	WZ $\eta$ $\lambda=1675.00$ , CuK $\alpha$ , $\lambda=1537.26$
" (E)	Fe (26)	Tungsten	Tungsten	WZ $\eta$ $\lambda=1675.00$ , FeK $\beta_1$ , $\lambda=1753.01$
" (F)	Fe (26)	Molybdenum	An oxide-coated platinum filament	CuK $\alpha_2$ , $\lambda=1537.26$ , FeK $\beta_1$ , $\lambda=1753.01$
" (G)	Mn (25)	Tungsten	Tungsten	FeK $\alpha_2$ , $\lambda=1932.08$ , FeK $\beta_1$ , $\lambda=1753.01$
" (H)	Cr (24)	Tungsten	Tungsten	MnK $\alpha_1$ , $\lambda=2097.51$ , FeK $\alpha$ , $\lambda=1932.08$

## (VI) Data and Results

The results obtained have been collected in Table II.

The long wave-length side of the white line is denoted by the letter  $k_l$ , and the short wave-length side of the same white line by  $k'_l$  ( $l=1, 2, 3, \dots$ ).

The wave-lengths are followed by the values of  $\frac{\nu}{R}$  and  $\sqrt{\frac{\nu}{R}}$ .

In this table may also be found the separation from the principal K-edge, expressed in wave-lengths, in  $\frac{\nu}{R}$ -units and also in volts.

Here the following physical constants were used.

$$\log 2d = 0.7823347 \quad (d = 2814.47 \text{ X. U. for calcite})$$

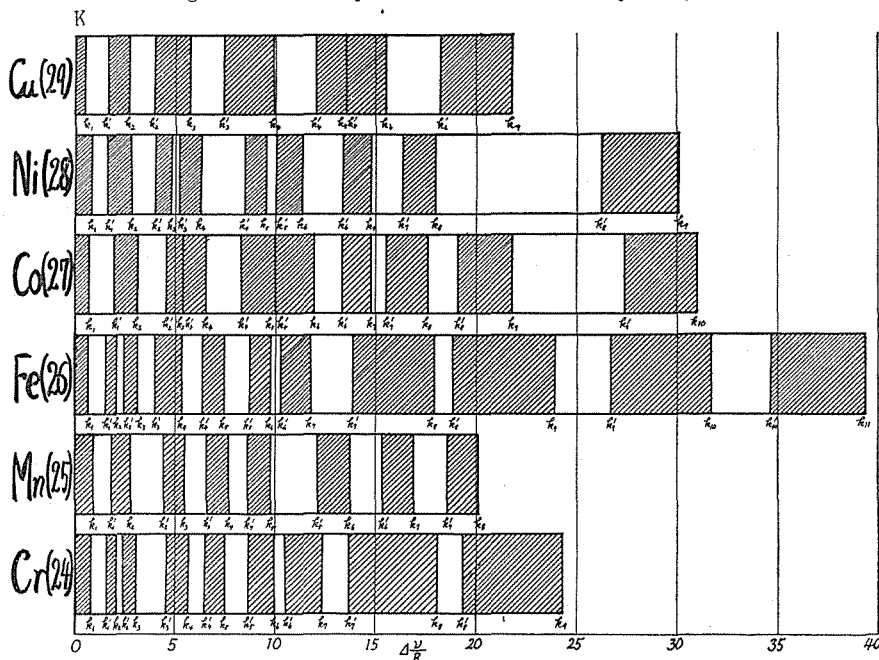
$$\log \frac{\nu}{R} = 5.9596469 - \log \lambda$$

$$V(\text{volts}) = 13.56 \times \Delta \frac{\nu}{R}$$

From the values of  $\Delta \frac{\nu}{R}$  in this table, the curves of Fig. 4 are constructed.

Fig. 4

Diagram of the multiple structure of the  $K$  absorption spectra.



In their general features, the results were nearly the same as those of B. Kievit and Lindsay,<sup>1</sup> although they did not give the results of measurement of the long wave-length side of the multiple structure.

The main new results here obtained are as follows.

I. NICKEL (29): Due to the appearance of the  $ZnK\alpha_{1,2}$  lines one edge reported by Kievit and Lindsay could not be found. But a new faint edge ( $k_3$ ) and a fairly strong edge ( $k_5$ ) were observed.

II. COBALT (27): The  $CuK\alpha_{1,2}$  radiations were very faint, so more edges ( $k_9$ ,  $k_{10}$ ) were observed than by Kievit and Lindsay. New edges ( $k_3$ ), ( $k_5$ ), ( $k_7$ ) were detected. Besides this plate, using a cobalt screen made by pouring a mixture of powdered cobalt and zapon enamel on a glass plate, two spectrograms were taken. The white lines given by this plate were narrower than those obtained with the metallic sheets. The main edge was very sharp. These changes might be ascribed to the oxidation of metallic cobalt in the powdered form.

1. B. Kievit and G. A. Lindsay, loc. cit.

Table II

The wave-lengths ( $\text{\AA}$ , U.), the values of  $\frac{\nu}{R}$  and  $\sqrt{\frac{\nu}{R}}$  for the multiple structure of the

	$K$	$k_1$	$k_1'$	$k_2$	$k_2'$	$k_2$	$k_2'$	$k_4$	$k_4'$	$k_6$	
Cu(29)	$\lambda$	1377.6	1376.7	1374.3	1372.1	1369.5	1365.9	1362.4	1357.4	1353.2	1350.1
	$\Delta\lambda$	0	0.9	3.3	5.5	8.1	11.7	15.2	20.2	24.4	27.5
	$\frac{\nu}{R}$	661.47	661.93	663.08	664.14	665.39	667.14	668.83	671.32	673.41	674.97
	$\Delta\frac{\nu}{R}$	0	0.46	1.61	2.67	3.92	5.67	7.36	9.85	11.94	13.50
	$\Delta\nu'$	0	6.2	21.8	36.2	53.2	76.9	99.8	133.6	161.9	183.1
	$\sqrt{\frac{\nu}{R}}$	25.72	25.73	25.75	25.77	25.80	25.83	25.86	25.91	25.95	25.98
Ni(28)	$\lambda$	1484.8	1482.9	1480.8	1477.9	1475.3	1473.4	1472.4	1469.8	1464.7	1462.1
	$\Delta\lambda$	0	1.9	4.0	6.9	9.5	11.4	12.4	15.0	20.1	22.7
	$\frac{\nu}{R}$	613.73	614.53	615.39	616.59	617.69	618.50	618.92	619.99	622.17	623.24
	$\Delta\frac{\nu}{R}$	0	0.80	1.66	2.86	3.96	4.77	5.19	6.26	8.44	9.51
	$\Delta\nu'$	0	10.8	22.5	38.8	53.7	64.7	70.4	84.9	114.4	129.0
	$\sqrt{\frac{\nu}{R}}$	24.77	24.79	24.81	24.83	24.85	24.87	24.88	24.90	24.94	24.96
Co(27)	$\lambda$	1605.2	1603.2	1599.7	1596.5	1592.5	1590.2	1590.2	1587.1	1582.3	1577.5
	$\Delta\lambda$	0	2.0	5.5	8.7	12.7	15.0	15.0	18.1	22.9	27.7
	$\frac{\nu}{R}$	567.69	568.39	569.65	570.79	572.23	573.05	573.05	574.19	575.93	577.66
	$\Delta\frac{\nu}{R}$	0	0.70	1.96	3.10	4.54	5.36	5.36	6.50	8.24	9.97
	$\Delta\nu'$	0	9.5	26.6	42.0	61.6	72.7	72.7	88.1	111.7	135.2
	$\sqrt{\frac{\nu}{R}}$	23.83	23.84	23.87	23.89	23.92	23.94	23.94	23.96	24.00	24.04
Fe(26)	$\lambda$	1740.1	1738.1	1735.2	1733.3	1731.9	1729.9	1727.0	1722.5	1719.3	1715.7
	$\Delta\lambda$	0	2.0	4.9	6.8	8.2	10.2	13.1	17.6	20.8	24.4
	$\frac{\nu}{R}$	523.68	524.29	525.18	525.75	526.16	526.79	527.67	529.03	530.02	531.13
	$\Delta\frac{\nu}{R}$	0	0.61	1.50	2.07	2.48	3.11	3.99	5.35	6.34	7.45
	$\Delta\nu'$	0	8.3	20.3	28.1	33.6	42.2	54.1	72.5	86.0	101.0
	$\sqrt{\frac{\nu}{R}}$	22.88	22.90	22.92	22.93	22.94	22.95	22.97	23.00	23.02	23.05
Mn(25)	$\lambda$	1893.9	1890.3	1887.0	1883.0	1876.7	1872.5	1868.3	1864.2	1860.4	1856.1
	$\Delta\lambda$	0	3.6	6.9	10.9	17.2	21.4	25.6	29.7	33.5	37.8
	$\frac{\nu}{R}$	481.17	482.09	483.01	483.94	485.58	486.66	487.74	488.84	489.83	490.96
	$\Delta\frac{\nu}{R}$	0	0.92	1.84	2.77	4.41	5.49	6.57	7.67	8.66	9.79
	$\Delta\nu'$	0	12.5	25.0	37.6	59.8	74.4	89.1	104.0	117.4	132.8
	$\sqrt{\frac{\nu}{R}}$	21.94	21.96	21.98	22.00	22.04	22.06	22.09	22.11	22.13	22.16
Cr(24)	$\lambda$	2066.3	2062.4	2058.8	2056.4	2055.2	2051.9	2045.1	2040.1	2036.4	2031.7
	$\Delta\lambda$	0	3.9	7.5	9.9	11.1	14.4	21.2	26.2	29.9	34.6
	$\frac{\nu}{R}$	441.03	441.86	442.62	443.14	443.40	444.10	445.59	446.68	447.50	448.53
	$\Delta\frac{\nu}{R}$	0	0.83	1.59	2.11	2.37	3.07	4.56	5.65	6.47	7.50
	$\Delta\nu'$	0	11.3	21.6	28.6	32.1	41.6	61.8	76.6	87.7	101.7
	$\sqrt{\frac{\nu}{R}}$	21.00	21.02	21.04	21.05	21.06	21.07	21.11	21.14	21.16	21.18

*K*-absorption limits and their separation from the principal *K*-edge  $\{\Delta\lambda, \Delta\frac{\nu}{K}, \Delta V(\text{volts})\}$

$k_5'$	$k_6$	$k_6'$	$k_7$	$k_7'$	$k_8$	$k_8'$	$k_9$	$k_9'$	$k_{10}$	$k_{10}'$	$k_{11}$
1350.1	1346.1	1340.7	1333.7								
27.5	31.5	36.9	43.9								
674.97	676.95	679.71	683.25								
13.50	15.48	18.24	21.78								
183.1	209.9	247.3	295.3								
25.98	26.02	26.07	26.14								
1461.0	1458.0	1453.3	1450.0	1446.3	1442.7	1423.9	1415.3				
23.8	26.8	31.5	34.8	38.5	42.1	60.9	69.5				
623.73	625.02	627.05	628.48	630.05	631.66	639.96	643.86				
10.00	11.29	13.32	14.75	16.32	17.93	26.23	30.13				
135.6	153.1	180.6	200.0	221.3	243.1	355.7	408.6				
24.98	25.00	25.04	25.07	25.10	25.13	25.30	25.37				
1577.5	1572.3	1568.4	1564.7	1562.5	1556.9	1553.0	1545.9	1531.4	1522.1		
27.7	32.9	36.8	40.5	42.7	48.3	52.2	59.3	73.8	83.1		
577.66	579.57	581.01	582.41	583.20	585.30	586.77	589.49	595.07	598.69		
9.97	11.88	13.32	14.72	15.51	17.61	19.08	21.80	27.38	31.00		
135.2	161.1	180.6	199.6	210.3	238.8	258.7	295.6	371.3	420.4		
24.04	24.07	24.10	24.13	24.15	24.19	24.22	24.28	24.39	24.47		
1711.7	1708.4	1706.7	1702.0	1695.4	1682.5	1679.7	1664.2	1655.9	1640.7	1632.1	1618.5
28.4	31.7	33.4	38.1	44.7	57.6	60.4	76.0	84.2	99.4	108.0	121.6
532.39	533.42	533.93	535.40	537.51	541.61	542.53	547.60	550.32	555.42	558.36	563.05
8.71	9.74	10.25	11.72	13.83	17.93	18.85	23.92	26.64	31.74	34.68	39.37
118.1	132.1	139.0	158.9	187.5	243.1	255.6	324.4	361.2	430.4	470.3	533.9
23.07	23.10	23.11	23.14	23.18	23.27	23.29	23.40	23.46	23.57	23.63	23.73
1847.4	1841.3	1835.3	1829.6	1823.4	1817.8						
46.5	52.6	58.6	64.3	70.5	76.1						
493.28	494.91	496.53	498.08	499.76	501.30						
12.11	13.74	15.36	16.91	18.59	20.13						
164.2	186.3	208.3	229.3	252.1	273.0						
22.21	22.25	22.28	22.32	22.36	22.39						
2026.4	2020.8	2018.2	2009.9	2004.0	1984.8	1979.5	1958.4				
39.9	45.5	48.1	56.4	62.3	81.5	86.8	107.9				
449.70	450.94	451.53	453.38	454.73	459.12	460.36	465.32				
8.67	9.91	10.50	12.35	13.70	18.09	19.33	24.29				
117.6	134.4	142.4	167.5	185.8	245.3	262.1	329.4				
21.21	21.24	21.25	21.29	21.32	21.43	21.46	21.57				

III. IRON (26): With a tungsten anticathode, the strong  $WZl$  line appeared in the structure, so another plate was taken with molybdenum as the anticathode. But no new result could be obtained. New edges detected are denoted by  $(k_{10})$  and  $(k_{11})$ .

IV. MANGANESE (25): A dozen plates were taken by various methods. A powder screen gave three or four secondary edges. Very thick screens gave no structure, and the main edge was very sharply limited and corresponded exactly to  $(K)$ . The diffuse edge obtained with some other plates with no structure corresponded to  $(k_1)$ . Some discrepancies were found between the multiple structure of pure manganese here obtained and that of Mn-Cu alloy reported by Kievit and Lindsay.

V. CHROMIUM (24): Powder screens gave the same results as in the case of manganese in powder form. Metallic screens gave a new edge  $(k_2)$ . Between  $(k_7')$  and  $(k_8)$  and also  $(k_8')$  and  $(k_9)$ , there are faint discontinuities but these could not be precisely located.

Through this work, the gradual falling in intensity at the short wave-length side of the black structure line (namely at the secondary edge) is a very peculiar feature of the spectrograms and is shown also in the microphotometric curves especially in cobalt.

## Part II, Theoretical Considerations

Several explanations to account for the origin of the extended multiple structure have been proposed by many investigators.

Here two reasonable hypotheses are taken into consideration.

The first hypothesis is that the multiple structure is the absorption discontinuities due to the absorption of a quantum of X-rays, resulting in the simultaneous ejection of many electrons from X-ray levels.

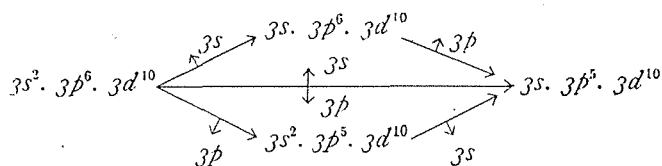
The second hypothesis is that the observed discontinuities are the  $K$ -ionization of an atom in which many electrons are lost owing to X-rays and photoelectrons from the same atom.

According to these hypotheses the following theoretical expectation for the wave-length or  $\frac{\nu}{K}$ -values of the multiple absorption edge can be made.

### (I) The Energy Values by the First Hypothesis

If the validity of the  $\{jj\}$  coupling can be accepted, the energy to remove two or more electrons simultaneously will be given approximately as follows:

Consider the change of state from a configuration..... $3s^2. 3p^6. 3d^{10}$  .....to the doubly ionized state..... $3s. 3p^5. 3d^{10}$ .....for example. Various modes of changing the state can be imagined: (i) a  $3s$  electron is removed, and then subsequently a  $3p$  electron; (ii) a  $3p$  electron is removed, and subsequently a  $3s$  electron is removed; (iii) a  $3s$  and a  $3p$  electron are simultaneously removed. These modes of ionization are shown diagrammatically in the following figure. The long arrows indicate the processes of ionization through which one state may be reached from another by removal of electrons.



Merely the simultaneous ionization is in question here, but because of its complicated structure this can not be directly calculated. But if we assume that the energy difference is determined by the initial and final states only as in Born's cyclic process, the energy is equal in these three cases, and the required one is most easily calculated by taking case (i). Under such consideration, the energy required to remove a *K* and an *M* electron simultaneously from the same atom will be approximately equal to the energy required to remove the *K* electron plus the energy required to remove an *M* electron from the atom with atomic number one unit greater. Symbolically this is expressed as follows

$$K(Z) + M(Z) \equiv \underline{KM(Z)} < KM(Z) \lesssim K(Z) + M(Z+1) \equiv \overline{KM(Z)} \quad (1)$$

where  $KM(Z)$  means the energy required to remove a *K* and an *M* electron simultaneously from an atom with an atomic number *Z*,  $K(Z)$  and  $M(Z)$  the energies required to remove the *K* and *M* electrons respectively, and  $\underline{KM(Z)}$  and  $\overline{KM(Z)}$  signify the probable lower and upper limits of the energy in question.

Similarly the energy  $M^2(Z)$  required to remove two *M* electrons from the atom will be given by

$${}_2M(Z) \equiv \underline{M^2(Z)} < M^2(Z) \lesssim M(Z) + M(Z+1) \equiv \overline{M^2(Z)}. \quad (2)$$

Following Wentzel<sup>1</sup>, let  $f_1, f_2, f_3, \dots$  be the number of electrons

1. G. Wentzel, Ann. d. Phys. **66**, 437 (1921)



in the  $K, L, M, \dots$  shell of the normal atom, then the energy of the atom will be given as a function of  $p_1, p_2, p_3, \dots$ .

Then we have

$$\begin{aligned} K(Z) &= W(p_1 - 1, p_2, \dots) - W(p_1, p_2, p_3, \dots) \\ &= -\frac{\partial W}{\partial p_1} + \frac{1}{2!} \frac{\partial^2 W}{\partial p_1^2} - \frac{1}{3!} \frac{\partial^3 W}{\partial p_1^3} + \dots \end{aligned} \quad (3)$$

and

$$\begin{aligned} M(Z) &= W(p_1, p_2, p_3 - 1, \dots) - W(p_1, p_2, p_3, \dots) \\ &= -\frac{\partial W}{\partial p_3} + \frac{1}{2!} \frac{\partial^2 W}{\partial p_3^2} - \frac{1}{3!} \frac{\partial^3 W}{\partial p_3^3} + \dots \end{aligned} \quad (4)$$

In general, let the notation  $K^{d_1} L^{d_2} M^{d_3}$  be the term values equivalent to the energy of an atom which has had  $d_1$  electrons removed from the  $K$  shell,  $d_2$  electrons removed from the  $L$  shell, and  $d_3$  electrons from the  $M$  shell and so on, then

$$\begin{aligned} K^{d_1} L^{d_2} M^{d_3} \dots &= W(p_1 - d_1, p_2 - d_2, p_3 - d_3, \dots) - W(p_1, p_2, p_3, \dots) \\ &= -\sum_i d_i \frac{\partial W}{\partial p_i} + \frac{1}{2!} \sum_{ik} d_i d_k \frac{\partial^2 W}{\partial p_i \partial p_k} \\ &\quad - \frac{1}{3!} \sum_{iki} d_i d_k d_l \frac{\partial^3 W}{\partial p_i \partial p_k \partial p_l} + \dots \end{aligned} \quad (5)$$

Using this result I derived the simple expression,

$$K M^n(Z) = K(Z) + n \left( M(Z) + \frac{\partial^2 W}{\partial p_1 \partial p_3} \right) + \frac{n(n-1)}{2} \frac{\partial^2 W}{\partial p_3^2}. \quad (6)$$

Although the values of  $\frac{\partial^2 W}{\partial p_1 \partial p_3}$ ,  $\frac{\partial^2 W}{\partial p_3^2}$  are unknown, this equation serves to clear the matter to some extent.

The vertical lines in Fig. 5 give the separation for the elements from Cu(29) to Cr(26) in  $\frac{\nu}{R}$ -units between the principal edge and the various secondary edges calculated according to the above principle.

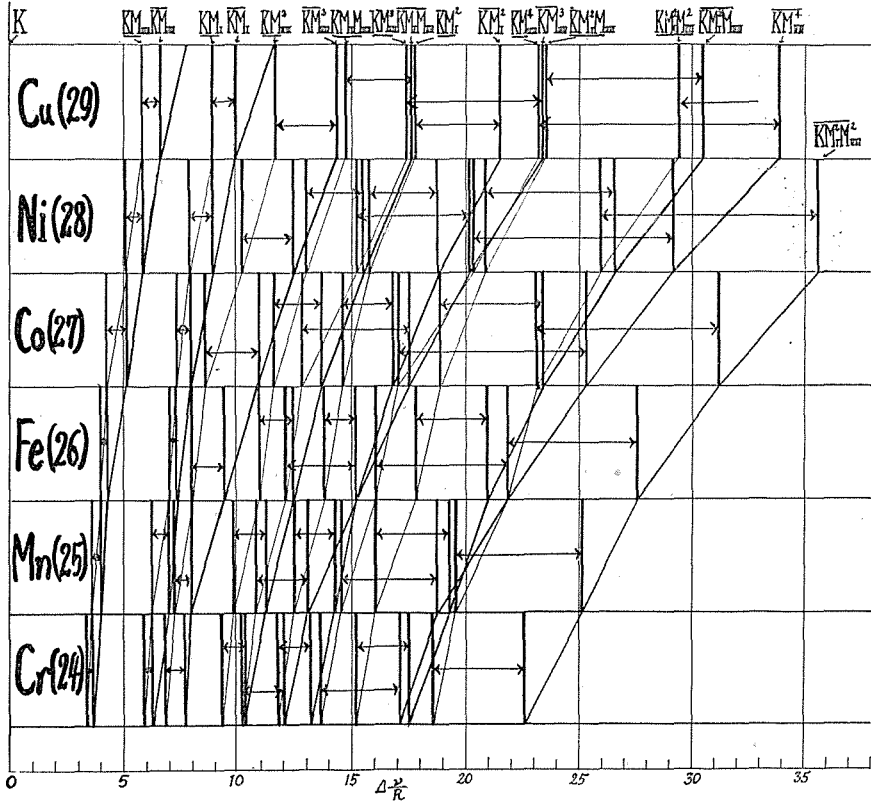
The value of the  $M$  levels in Fig. 5 are taken from the paper by E. C. Stoner<sup>1</sup>, who has calculated the term values using Thoraues'<sup>2</sup> data. The values for Ga(30) are calculated by interpolation from Mosley's diagram.

1. E. C. Stoner, Phil. Mag. 2, 97 (1926)

2. Thoraues, Phil. Mag. 1, 312 (1926)

Fig. 5

Calculated energy level diagram for multiple X-ray ionization.



(II) The Energy Values by the Second Hypothesis

This hypothesis regards the observed structure as due to the ejection of a *K* electron from the multiply ionized atom in various shells.

Let  $K^i(Z)$  be the energy required to eject a *K* electron from the singly ionized atom in the *L* shell, then we have as a first approximation.

$$K^i(Z) < \overline{K^i(Z)} = K(Z) + L(Z+1) - L(Z). \quad (7)$$

Similarly let  $K^{i^2}(Z)$  be the *K* ionization potential for the doubly ionized atom in the *L* shell,

$$K^{i^2}(Z) < \overline{K^{i^2}(Z)} = K(Z) + L(Z+2) - L(Z). \quad (8)$$

Following Wentzel<sup>1</sup>, I have

$$KL^m(Z) \equiv KL^m - L^m = K + m \frac{\partial^2 W}{\partial p_1 \partial p_2}.$$

Let the total energy of the normal atom be equal to

$$W = - \sum_k p_k \frac{\left( Z - \sum_{i=1}^{k-1} p_i - s_k \right)^2}{k^2}, \quad (9)$$

where  $s_k$  is a screening constant, and we obtain the formula:

$$\frac{\partial^2 W}{\partial p_1 \partial p_n} = \frac{2}{n} \left\{ \frac{\left( Z - \sum_{i=1}^{n-1} p_i - s_n \right)}{n} - \frac{p_n}{n} \frac{\partial s_n}{\partial p_n} - n \sum_{k=n+1} \frac{p_k}{k^2} \right\}. \quad (10)$$

For example,

$$\frac{\partial^2 W}{\partial p_1 \partial p_2} = \left\{ \frac{Z - p_1' - s_2}{2} - \frac{p_2}{2} \frac{\partial s_2}{\partial p_2} - \frac{2p_3}{3^2} - \frac{2p_4}{4^2} \right\}, \quad (11)$$

for the atom of the iron group ionized in the shell  $2p$ . Here  $p_1'$  contains the  $p$  of  $1s$  and  $2s$ .

The first term of the right hand side of the equation is obtained from the value of  $\sqrt{\frac{\nu}{R}}$  of  $L_{II}(Z)$  of the atom in question as a first approximation<sup>2</sup>.

The value of  $\frac{\partial s_2}{\partial p_2}$  is 0.5 also as a first approximation. This is correct for a spherical shell at least.

The values of  $\frac{\partial^2 W}{\partial p_1 \partial p_2}$  computed from this equation are respectively

2.06, 2.30, 2.45, 2.60, 2.74, and 2.77 in  $\frac{\nu}{R}$ -units for Cr, Mn, Fe, Co, Ni, and Cu respectively.

And these figures give the values of separation from the principal  $K$ -edge.

The values (designated by  $\overline{KL} - K$ ) and the values of  $\overline{K'L} - K$  and  $\overline{K'L^2} - K$  computed from equations (7) and (8) respectively, are plotted in Fig. 6.

The term  $KL$  ( $1s, 2s^2, 2p^6$ ) will be  $^1P$  and  $^3P$ .

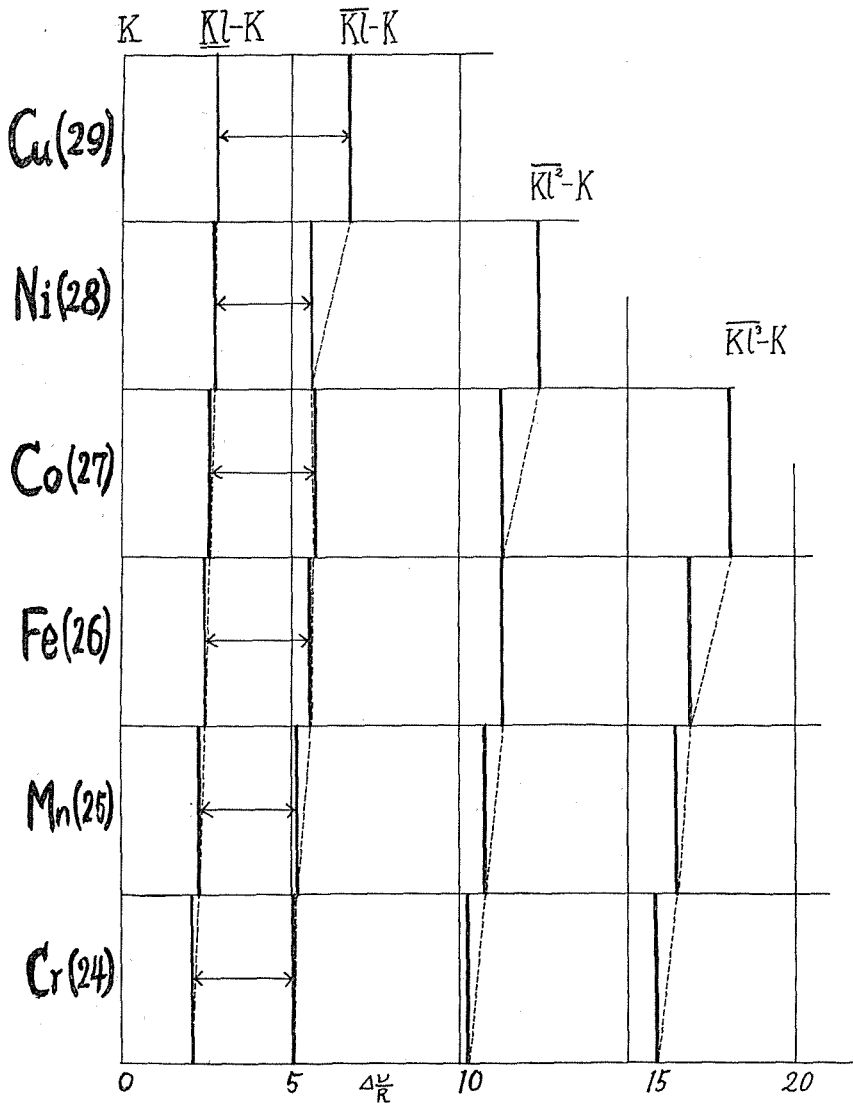
Real value will exist between  $\overline{K'L} - K$  and  $\overline{K'L^2} - K$ , or very close to them.

1. G. Wentzel, l. c.

2. This point will be discussed elsewhere.

Fig. 6

The theoretical value of separation. The  $K'$  edge of an atom that has lost one or more  $2p$  electrons—The principal edge.



(III) Remarks

By the preceding line of argument, only approximate values can be secured for the energy levels. Hence the more detailed points which must be taken into consideration will be mentioned here.

(1) *Change of term values with the coupling between electrons*

It has been assumed that the  $\{jj\}$  coupling may hold true, but this is not always the case.

For electrons of the same group in light elements, the  $\{LS\}$  coupling may occur. Under these circumstances, if a  $K$ -electron and two  $M_{II,III}(3p)$  electrons are ejected from an atom, there will be present various levels deviating from the value  $KM_{II,III}^2(Z)$ , because even if the coupling between  $K$  and  $M$  electrons may be  $\{jj\}$ , that between two  $3p$  electrons may be recognized as approaching the  $\{LS\}$  coupling, which will give rise to fairly widely separated energy levels such as  $^1S_0$ ,  $^1D_2$ , and  $^3P_{0,1,2}$ . Recently S. Goudsmit<sup>1</sup> derived the expressions giving the change in the positions of the energy levels with change in electron coupling for the configuration  $p^4$ . Applying his theory in the case of X-rays, I attempted some estimations. As an example, for nickel, the triplet separation must be equal to 0.16 in  $\frac{\nu}{R}$ -units. Let the separation between  $^1S_0$  and  $^3P_{0,1,2}$  or  $^1D_2$  and  $^3P_{0,1,2}$  become ten times this triplet separation, then the total separation will become 1.6. But the coupling strength cannot be accurately obtained and this is only a rough estimation. But these values will deviate fairly far from that of a single  $KM_{II,III}^2$  term. Hence there is a possibility that *many* absorption edges will be *experimentally* secured from one configuration of electrons.

(2) *The end orbits of electrons in the process of absorption*

In contrast to Kievit and Lindsay, in the foregoing discussion I have assumed that the electrons are completely taken from the atom, taking into consideration the fact that the ionization potential of the metallic element is small. Actually in the case of a metal in the solid state, there are free electrons present, and we cannot predict how many and which electrons are free. Accordingly we cannot precisely decide whether a metal consists of atoms or ions. Hence the determination of the end orbit is especially difficult. But this can be done in the case of gaseous atoms, using optical data. One word more may be said in connection to this point. It is known that for every valency electron  $i$  ( $i=1, 2, 3, \dots$ ) that takes part in the change of state of the atom the selection rule for  $l$  is  $\sum_i \Delta l_i = \pm 1$ , and not  $\Delta l_i = \pm 1$ . In the case of X-ray spectroscopy, if we can obtain the multiple structure of the absorption spectra in gaseous atoms, and can

1. S. Goudsmit, Phys. Rev. **35**, 1325 (1930)

accurately determine it, it will be interesting to test whether the above selection rule holds or not also in the process of absorption in the X-ray region.

(3) In constructing Fig. 6 only  $3s$  and  $3p$  electrons were taken into consideration and  $3d$  or  $4s$  electrons were neglected. This must cause slight discrepancies between the calculated and the observed values.

### Conclusion

In spite of the presence of the above-cited difficulties, there are some facts explained qualitatively at least. Comparison of Fig. 4 and Fig. 5 shows that coincidence of the value is frequently found. The intersections of the curves  $\overline{KM}_I^2$  and  $\overline{KM}_{II, III}^2$ ,  $\overline{KM}_I^2 M_{II, III}$  and  $\overline{KM}_{II, III}^4$  are interesting, and the irregularities that are found in the case of Fe and Mn in Fig. 4 can be predicted.

The fact that a gradual decrease in intensity towards the short wave-length side is often observed in many spectrograms, can be interpreted by the idea of multiplets in the case of  $\{LS\}$  coupling.

In comparing Fig. 4 and Fig. 6, one of the edges ( $k_2$ ), ( $k_3$ ) ( $k_4$ ), and ( $k_5$ ) is to be regarded as due to a singly ionized atom in  $L$  shell. The facts that the related black lines of similar intensity and structure nearly fall into the same vertical lines in Fig. 4 (that is variations with the atomic number are small), and that there is a gradual fall in intensity at the short wave-length side, are due to the term multiplicities of  $^1S$  and  $^3S$  for the configuration  $1s\ 2s\ 2p^6$  and  $^1P, ^3P$  for  $1s\ 2s^2\ 2p^5$  and so on. The precise theoretical determination of the energies required for multiple ionization of the atom is difficult, but the probable explanation seems to be provided by these two hypotheses to some extent. So on the whole, it is to be supposed that in the process of absorption of X-rays these two different types of absorption really occur, and that the spectrograms are the result of superposition of such a complex process.

But here arises two questions of probability :

- (1) The probability of multiple electron jumps owing to the absorption of a single quantum.
- (2) The probability of the atom being brought into the state of multiple ionization by X-rays and photoelectrons from the same atom, and especially the length of stay (Verweilzeit).

The problem should be solved by the new quantum mechanics, and this is intimately related to the explanation of the spark lines in the X-ray emission spectra.

In conclusion, the writer wishes to express his sincere thanks to Prof. M. Ishino for his kind guidance and for the interest he has taken in this research.

---

Plate Figure

Fig. 2. Multiple structure in the  $K$  absorption spectra of metallic elements (A)–(H)

